Autonomous Adaption of Intelligent Humidity-Programmed Hydrogel Patches for Tunable Stiffness and Drug Release

*Stephan Pflumm, Yvonne Wiedemann, Dominik Fauser, Javidan Safaraliyev, Dominique Lunter, Holger Steeb, and Sabine Ludwigs**

Intelligent humidity-programmed hydrogel patches with high stretchability and tunable water-uptake and -release are prepared by copolymerization and crosslinking of *N*-isopropylacrylamide and oligo(ethylene glycol) comonomers. These intelligent elastomeric patches strongly respond to different humidities and temperatures in terms of mechanical properties which makes them applicable for soft robotics and smart skin applications where autonomous adaption to environmental conditions is a key requirement. It is shown that beyond using the hydrogel in the conventional state in aqueous media, new patches can be controlled by relative humidity. This humidity programming of the patches allows to tune drug release kinetics, opening potential application fields such as skin wound therapy and personalized medication. In situ dynamic-mechanical measurements show a huge dependence on temperature and humidity. The glass transition temperature T_g shifts from around 60 °C at dry conditions to below 0 °C for 75% r.h. and higher. The storage modulus is tunable over more than four orders of magnitude from 0.6 up to 400 MPa. Time-temperature superposition in master curves allows to extract relaxation times over 14 orders of magnitude. With strains at break of over 200% the patches are compliant with human skin and therefore patient-friendly in terms of adapting to movements.

1. Introduction

Highly flexible organisms such as Octopus have led to the emerging field of soft material robotics with manifold applications in wearable electronics, biomedicine, microfluidics, soft sensor, and actuator devices.[1–5] While rigid materials with discrete joints already allow for precise, predictable robotic systems nowadays, natural systems still outperform man-made devices in many aspects including conforming to and interacting with their environment. Connecting soft materials with humans has become a cross-disciplinary topic for materials science with polymers being the most promising material class. Especially low modulus elastomers such as poly(dimethylsiloxane) (PDMS) and commercial products such as Ecoflex and Dragonskin find the interest of the soft robotic engineering community,[6,7] however these materials are passive and not stimuli-responsive.

For the interfacing of novel intelligent materials with human skin, soft and flexible materials are required to match the properties of human skin which are not trivial: their elastic moduli should be below the elastic modulus of skin (in the order of 15–200 MPa) and stretchability of over 100% is favorable, furthermore the materials should be biocompatible, tissue-compliant (e.g., toward wounds), and easy to handle at ambient conditions.[8–10] For personalized drug therapies, the patches have to additionally take up and release drugs in a controllable and reliable fashion.

In this context, smart or stimuli-responsive materials are ideal because they show a controlled response to changing environmental conditions.[11–13] The concept of hydrogels for drug delivery has been highlighted, e.g., by Peppas et al.[14] For biomedical applications, often poly(*N*-isopropylacrylamide) (PNIPAM)-based materials are applied, because they show a volume phase transition around 32 °C (which is related to the lower critical solution temperature[15] of the homopolymer), which is close to human body temperature,[16] and they exhibit good biocompatibility.[17] Their rather sharp transition makes thermosensitive PNIPAM-hydrogels attractive for on-demand drug release applications. Besides using *N,N'*-methylenbisacrylamid as typical crosslinker,[18] poly(ethyleneglycol) (PEG)-based

S. Pflumm, J. Safaraliyev, S. Ludwigs
IPOC – Functional Polymers
Institute of Polymer Chemistry
University of Stuttgart
Pfaffenwaldring 55, 70569 Stuttgart, Germany
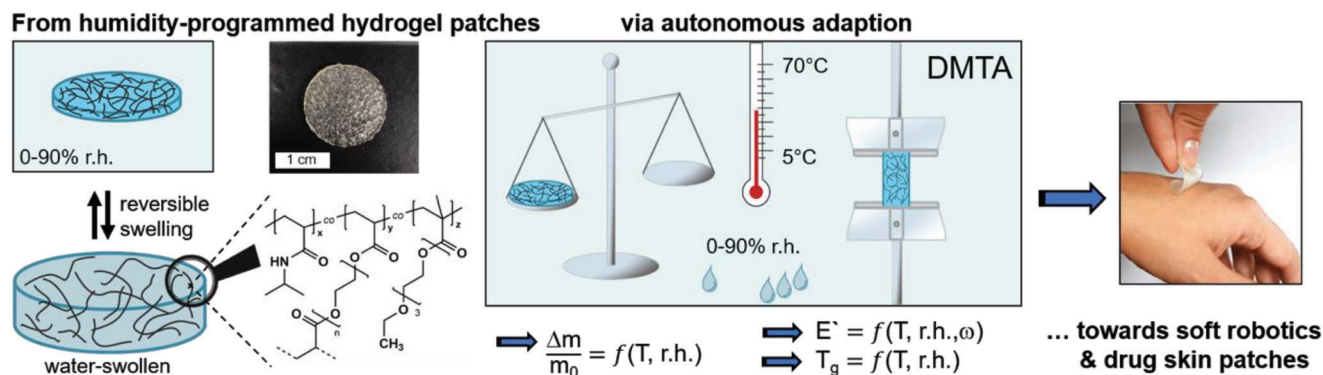E-mail: sabine.ludwigs@ipoc.uni-stuttgart.de

Y. Wiedemann, D. Lunter
Pharmaceutical Technology
Institute of Pharmacy and Biochemistry
University of Tuebingen
Auf der Morgenstelle 8, 72076 Tuebingen, Germany

D. Fauser, H. Steeb
Institute of Applied Mechanics (Civil Engineering) & SC SimTech
University of Stuttgart
Pfaffenwaldring 7, 70569 Stuttgart, Germany

Scheme 1. Strategy of the manuscript, from left to right. Sketches and chemical structure of hydrogel patches (NIPAM:PEG-DA:TEG-MA with $x{:}y{:}z$ = 70:10:20 mol%), the photo shows a patch at ambient conditions. From water (vapor) sorption experiments, the water content is measured as function of temperature (T) and relative humidity (r.h.). DMTA is applied to obtain the stiffness E' and the glass transition as function of T, r.h., and frequency (ω). Ultimately, the patches shall be applied in soft robotics and as skin patches for controlled drug release.

crosslinkers have been shown to enhance the swelling ratio and biocompatibility of the hydrogels.[19,20] Here, the influence of crosslinking density and molecular weight of the PEG is of major importance for the diffusion characteristics which is needed for drug uptake and release.[21] Recent smart hydrogel devices include small-scale hydrogel adhesive robots[22] and 3D-printed smart structures by two-photon-polymerization-based 3D microprinting.[23] Aiming toward mechanical robustness of hydrogels in the water-swollen state,[24–26] the combination of high swellability and stretchability was, e.g., tackled by nanostructured hydrogels.[27]

It is a common phenomenon that the hydrogels are typically hard and brittle at ambient conditions, i.e., in the dry state. Studies on manipulation by relative humidity and temperature, mimicking environmental conditions, are far less studied than in-water applications. Reversible switching by humidity was, e.g., demonstrated in hydrogel-actuated nanostructures within high-aspect ratio silicon nanocolumns by Sideronko et al.[28] Lv et al. reported on the humidity responsiveness of photopolymerizable PEG-DA hydrogels and visualized their use as "humidity test strips" and walking devices.[29] Photogated humidity-driven motility was shown by Naumov and co-workers.[30] An interesting effect was reported for freeze-dried PNIPAM-based thermoresponsive hydrogels which absorb moisture and are able to ooze/condense to liquid water.[31]

Systematic studies on relating macroscopic mechanical behavior and moisture uptake remain rarely addressed in the literature. Typically mechanical properties are only compared as function of crosslinking density[32] and stress–strain curves are studied as function of relative humidity.[25] Humidity-sensitive conducting polymer films with applications to linear actuators[33] and bilayer actuators based on poly(ethylenedioxythiophene):poly(styrene sulfonate) (PEDOT:PSS) were shown by Taccola et al.[34] and our own group.[35] Due to the presence of the polyelectrolyte PSS, these systems are highly hygroscopic and we found that the elastic moduli and volumetric strains of bilayers can be tuned over several orders of magnitude by altering the relative humidity and therefore environmental conditions.[35]

We here report on the humidity- and temperature-responsive mechanical behavior of elastomeric hydrogels which are stable from the fully dry to fully water-swollen states. The novel intelligent hydrogel material is obtained by copolymerization and crosslinking of N-isopropylacrylamide (NIPAM) and oligo(ethylene glycol) comonomers.

Scheme 1 summarizes the main strategy of the manuscript. The patches have excellent water-uptake and water-release abilities and can be reversibly swollen and deswollen from ambient conditions (i.e., from 0 to 90% relative humidity at room temperature) to the fully water-swollen state. We find a linear dependence of the water uptake from the temperature, in the wet and over the whole relative humidity range in equilibrium, as measured by water (vapor) sorption measurements. Dynamic mechanical temperature analysis (DMTA) is used to measure the mechanical behavior as function of temperature, relative humidity, and the frequency. Elastic moduli ranging from 0.6 up to 400 MPa are obtained as function of temperature and relative humidity, this corresponds to four orders of magnitude for the very same material. The glass transition temperature T_g can be varied from around 60 °C at dry conditions to temperatures below 0 °C for 75% r.h. and higher.

Moisture uptake is shown to have a major effect on the mechanical properties by softening and reducing stiffness. In the humid state, the materials behave like smart rubbers which can autonomously adapt to their environment and are therefore applicable in soft-robotics devices. We further show that drug-loaded hydrogel patches can be programmed at different relative humidities which reveal tunable release kinetics and are promising for wound healing in personalized medication.

2. Results and Discussion

The hydrogel patches were prepared by photo-induced radical polymerization of NIPAM and poly(ethylene glycol)-diacrylate (PEG-DA) as crosslinker and triethyleneglycolmonoethylethermethacrylate (TEG-MA) which shall act as grafted chains and have a softener effect. The final ratio of NIPAM:PEG-DA:TEG-MA in the material was 70:10:20 mol%. After washing and drying, the patches were characterized by IR-spectroscopy, elementary analysis, and thermogravimetric analysis (TGA), confirming the successful incorporation of the monomers into the
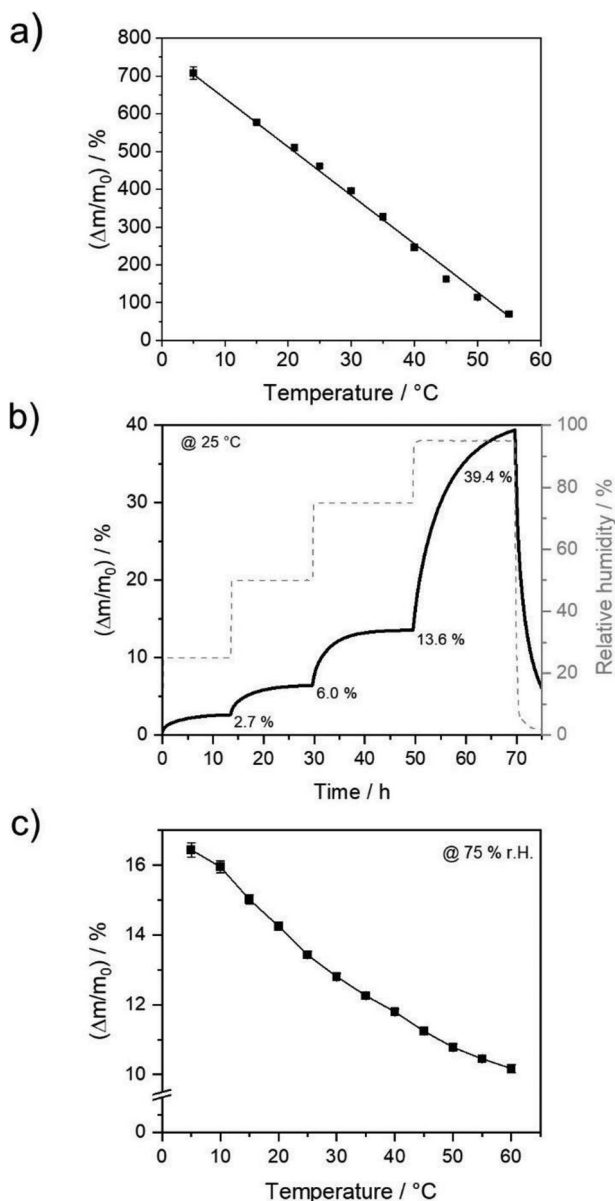
2300937 (2 of 9)

ADVANCED
SCIENCE NEWS
www.advancedsciencenews.com

ADVANCED
MATERIALS
TECHNOLOGIES
www.advmattechnol.de

a)

b)

c)

Figure 1. a) Equilibrium swelling degree as function of temperature after 24 h in water (black line: linear fit with R^2 of 0.993). b) Average, time-dependent water uptake at 25 °C and different relative humidity. c) Average equilibrium water uptake as function of temperature at 75 % r.h.

crosslinked hydrogel, see Figures S1 and S2 and Table S1 in the Supporting Information. The patches were then characterized in terms of their water-swelling capabilities in water and at controlled relative humidities as function of temperature.

Figure 1a shows the equilibrium swelling degree of the hydrogel after storing the samples in water for 24 h. The water uptake is calculated according to Equation (1) with m_0 as mass of the vacuum-dried hydrogel and m_s as the mass of the swollen hydrogel

$$\text{Water uptake} = \frac{\Delta m}{m_0} = \frac{m_s - m_0}{m_0} \times 100\% \qquad (1)$$

The highest water uptake of over 700% is found at 5 °C. With increasing temperature, the water uptake linearly decreases to around 70% at 55 °C. At 25 °C, the equilibrium degree of swelling is 461%. This linear relationship between the water uptake and the temperature is unusual for PNIPAM-bearing materials which typically show a well-pronounced volume phase transition.[36] The differential scanning calorimetry (DSC) analysis shows no clear phase transition (neither in the swollen nor in the dry state). The TGA showed degradation starting at around 390 °C (Figure S2, Supporting Information). The linear water uptake characteristics in the equilibrium seem to be therefore dominated by the presence of 10 mol% PEG-DA as crosslinker in the hydrogel. In general, PEG-based materials are very hygroscopic and have excellent water-binding capabilities.[37–39] To further elucidate this finding, DSC measurements and swelling experiments of materials with less than 10 mol% PEG-DA as crosslinker were performed, Figure S4, Supporting Information. With decreasing PEG-DA content, the materials show more defined volume phase transitions and stronger swelling degrees at the volume phase transition, i.e., they become more PNIPAM-hydrogel-like, see discussion in the Supporting Information. Interestingly, in the nonequilibrated state upon fast heating, our materials do show a more pronounced volume phase transition between 30 and 40 °C, see Figure S5 in the Supporting Information. This phenomenon will be studied in more detail in a future study. In the current manuscript, only the equilibrated states of the hydrogel are of interest.

Figure 1b shows the water uptake upon increase of the relative humidity in a step-wise fashion at 25 °C, as obtained from dynamic vapor sorption measurements. The increase with respect to the dry state amounts to 2.7% at 25% r.h., 6.4% at 50% r.h., 13.6% at 75% r.h., and over 39% at 95% r.h. (**Table 1**). The most significant water absorption happens from 75% to 95% r.h. at 25 °C, please note that the sample is not in sorption equilibrium at the highest r.h. A typical sorption isotherm is provided in Figure S6 in the Supporting Information, which suggests a type III classification,[35,40] as there is no shoulder at lower r.h. and therefore no identifiable monolayer formation. Dynamic vapor sorption experiments were also performed at 5 and 60 °C for different r.h., Figure S7 in the Supporting Information. Representatively, the temperature influence at 75% r.h is shown in the temperature range of 5 to 60 °C, Figure 1c. While at 5 °C the average water uptake is 16.4 ± 0.2%, it reduces to 10.2 ± 0.1% at 60 °C. As the temperature is increased, the samples absorb less water in a nearly linear fashion. The characteristic quasi-linear behavior of temperature-dependent swelling and deswelling in water is reflected in the temperature-dependent water absorption in humid atmospheres as well.

The reversible uptake and release of water (liquid and vapor) motivated us to test the abilities of the new material for drug-loading and -release. As model system diclofenac sodium was chosen as water-soluble active pharmaceutical ingredient. The loading is performed by swelling the hydrogels for 24 h in a diclofenac sodium solution (concentration: 2.5 g L⁻¹) at 25 °C. A similar linear dependency between the drug/water uptake and the temperature was observed, only slightly higher degrees of swelling were obtained which we ascribe to the ionic drug, i.e., ionic strength.[41] The drug-release analysis is performed by loading the drug-loaded water-swollen hydrogel on top of a

Table 1. Water uptake, storage modulus E', and T_g (obtained by maximum of tan δ) for selected measurement conditions. Note that values marked with * were not in sorption equilibrium.

r.h. [%]	Equilibrium water uptake [%]			E' [MPa]			T_g [°C]
	5 °C	25 °C	60 °C	5 °C	25 °C	61 °C	
0	0	0	0	388.9 ± 133.7	128.0 ± 10.1	7.9 ± 1.6	59 ± 2
25	2.5 ± 0.0*	2.7 ± 0.1	2.2 ± 0.0	227.7 ± 60.9	29.8 ± 2.9	1.3 ± 0.0	36 ± 2
50	6.0 ± 0.3*	6.4 ± 0.1	5.3 ± 0.0	78.3 ± 16.5	4.4 ± 1.2	0.7 ± 0.1	21 ± 2
75	12.1 ± 0.8*	13.6 ± 0.1	10.2 ± 0.1	3.6 ± 0.8	0.7 ± 0.1	0.4 ± 0.0	–
95	–	39.4 ± 0.1*	–	–	0.5 (@ 90%)	/	–
in H$_2$O	708 ± 16	461 ± 4	69 ± 2 (@ 55 °C)	–	–	–	–

membrane in a Franz diffusion cell which is separated into a donor and an acceptor compartment, **Figure 2**a. The acceptor compartment is filled with a phosphate buffered saline (PBS) that mimics tissue fluid, the membrane mimics the skin. The drug release into the acceptor medium was studied at 32 °C. This method is well accepted in the literature because it allows an assessment of the release behavior of patches when applied to the skin.[42] As proof of concept, the experiment was performed using the hydrogel patch in the water-swollen state. This means the hydrogel is over the whole experimental period in contact with

the aqueous acceptor medium and therefore the drug is released through a diffusion process from the hydrogel into the acceptor medium, Figure 2a top. Figure S8 in the Supporting Information shows the corresponding release profile. More interesting is the release from patches which were conditioned at different r.h., Figure 2a bottom. The patches were again loaded from drug-containing aqueous solutions and afterward programmed at different humidities, namely, at 25%, 50%, and 75% r.h. Please note that during this conditioning the patches dry by losing water by evaporation, but retain the drug inside the hydrogel network. The
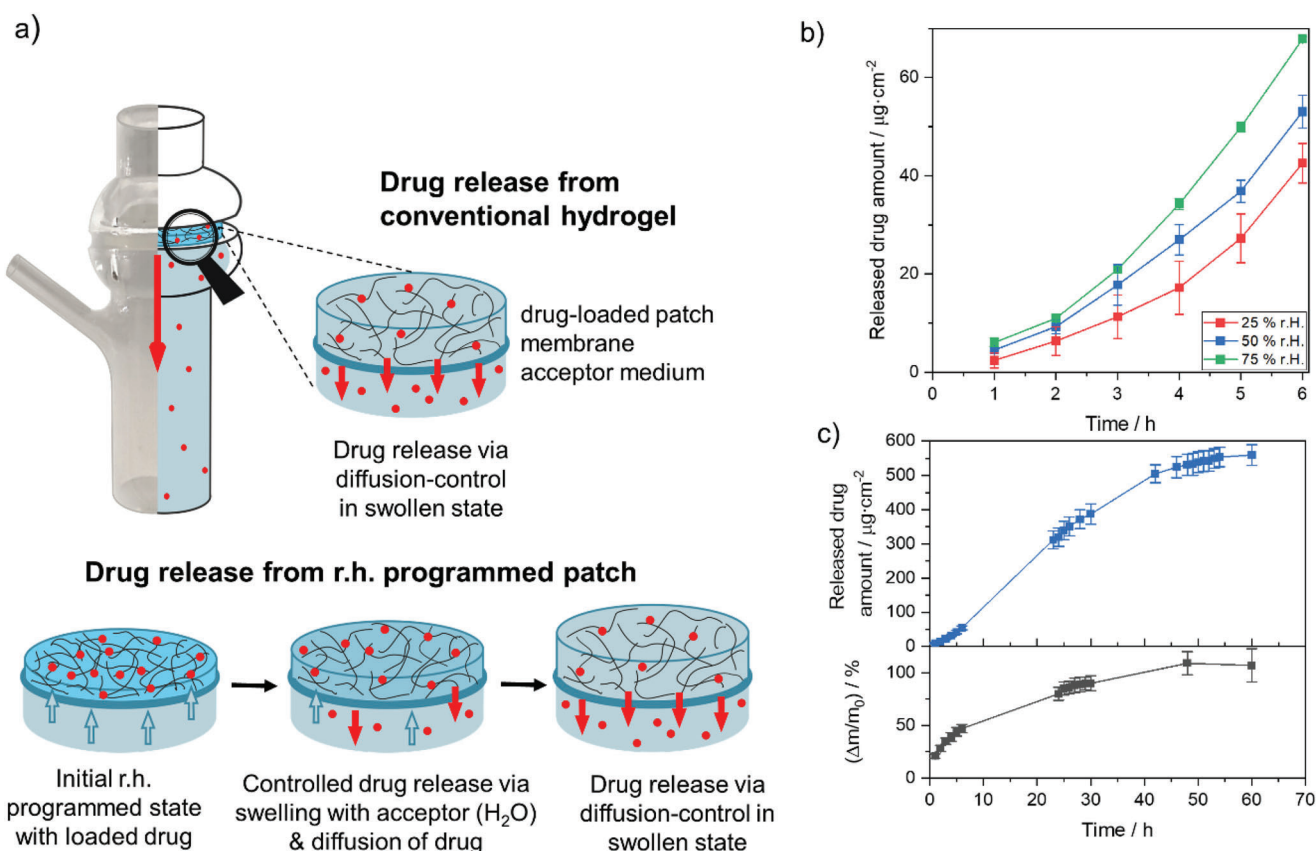

Figure 2. a) Sketch showing a Franz diffusion cell which is used to study drug release from using the patch as conventional water-swollen hydrogel and from r.h. programmed patches. b) Drug release out of a hydrogel which was conditioned at different r.h. over a period of 6 h. c) Drug release over 60 h with drug-loaded material conditioned at 50% r.h. together with the swelling degree of drug-loaded hydrogel during drug release.

**ADVANCED
SCIENCE NEWS**

www.advancedsciencenews.com

**ADVANCED
MATERIALS
TECHNOLOGIES**

www.advmattechnol.de

cumulative amounts of diclofenac sodium released from the programmed patches during the first 6 h are shown for the three different relative humidities in Figure 2b. The higher the humidity at which the patches were conditioned, the higher the release rate at the respective time during the period of 6 h. While the patches which were equilibrated at 25% r.h. show a drug release of ≈43 µg cm^{-2} after 6 h, this was almost doubled with an amount of ≈68 µg cm^{-2} released from 75% r.h. equilibrated patches. This is a very interesting finding because it means that the drug release can be tuned by the conditioning process in r.h.

When extending the release experiment over a period of 60 h, a sigmoidal progression was found, Figure 2c top, a plateau can be seen after around 50 h of the measurement. The change in swelling degree was monitored in parallel to the measured amount of released drug, Figure 2c bottom. After a steep initial increase in the swelling degree, a linear increase can be detected, which after ≈50 h reaches a plateau in the swelling degree. This behavior can be explained by the transmembrane PBS diffusion from the acceptor compartment of the Franz diffusion cells that causes—similarly to the water uptake experiments above—the swelling of the r.h. programmed hydrogel patches. The underlying mechanism seems to be a complex interplay between the swelling with acceptor medium and diffusion of drug from the patch into the acceptor medium. The drug release is strongly influenced by the original r.h. programmed state and the resulting swelling process as function of time. Only in the fully swollen state (after ≈50 h) the drug-release becomes diffusion-controlled and resembles the conventional drug release from the water-swollen state. The release profile may be explained by the polymer chain relaxation within the network as a result of swelling, whereby the mesh size increases which leads to enhanced diffusivity of the drug.[43] For mesh size analysis from the water content measurements, we refer to Figure S3 in the Supporting Information. The drug release rate is strongly influenced by the degree of swelling from the original r.h. programmed state, which then has a strong influence on the mobility of the drug molecules in the network and its release kinetics.[44,45] To further understand this phenomenon, we are currently performing a detailed drug release kinetics study which will be published in a separate study.

Here, our highlight is that moisture absorption from the environment can be used to adjust and control release rates. It implies that the hydrogel patches can self-control their release as a function of moisture as it may be present, e.g., in a wound. The Franz cell is mimicking the situation of a wound where wound exudate is released. This wound exudate will then—similar to the PBS—lead to a swelling of the patches and induce the release process. The patch would thus autonomously regulate the drug release depending on the amount of wound exudate. An additional advantage is that the drug is enclosed in the humidity-programmed hydrogel networks and gets only released when brought in contact with the tissue fluid. The drug is released on-demand and autonomously adapting to the moisture in the wound.

In terms of mechanical compliance and suitability for skin patch applications, the mechanical properties of the materials were studied in detail. Uniaxial tensile tests of the patches were performed at finite deformations at ambient conditions, **Figure 3**a. The experiments were performed under static conditions

(10 mm min^{-1}). The stress–stretch response shows a distinct S-shape hyperelastic behavior up to $\lambda > 3$ with $\lambda = \frac{l}{l_0}$. This corresponds to a strain-at-break ϵ_b above 200% ($\epsilon = \frac{l-l_0}{l_0} \times 100\%$). To fit the data points of the S-shape curve, the hyperelastic eight-chain model of Arruda and Boyce was applied (see the Supporting Information for further Information). The inherent two effective material parameters of the eight-chain model were fitted using the nonlinear least-square Levenberg–Marquardt algorithm. The fit suggests that there must be a reorientation and stretching of the polymer chains in loading direction within the crosslinked network which is typical for hyperelastic polymers.[46] The data underline the fact that the hydrogel has great flexibility and stretchability and is compliant with human skin which has usually strains-at-break around 100%.[9,10]

Going beyond applications as skin patches, it is also important to understand the properties in terms of stiffness. Targeting for the unique behavior of the patches to react to temperature and relative humidity, a systematic mechanical characterization was conducted with a dynamic mechanical analysis apparatus. This included the relative humidity range from 0% to 90% and temperatures between 5 and 73 °C. First, amplitude sweeps were carried out to ensure working in the linear viscoelastic regime (see Figure S10 and Table S2 in the Supporting Information for further information). In the following frequency sweeps, the force amplitudes were adapted accordingly.

Figure 3b shows the storage modulus E' measured at different relative humidities in the temperature range of 5 up to 73 °C. At dry conditions (0% r.h., black curve), E' has the overall highest values and evolves from around 390 MPa down to 3 MPa with increasing temperature, which corresponds to two orders of magnitude. This trend is also seen for 25% (red curve) and 50% r.h. (blue curve). In more humid conditions at 75% r.h., E' is reduced from around 4 to 0.4 MPa, i.e., the storage modulus is much less influenced by the temperature compared to drier conditions. From the graphs, one can clearly see that the influence of the r.h. at constant temperature is significant. At 25 °C, the storage modulus decreases from about 130 MPa (0% r.h.) over 30 MPa (25%) to 4 MPa (50%) down to below 1 MPa (75%). Please note that further increasing the r.h. to 90% does lead to E' of 0.5 MPa, which makes us conclude that above 75% r.h. no further changes are obtained. To bring the storage moduli in context of other soft materials, e.g., PDMS, values below 1 MPa are typical for crosslinked elastomeric materials.[35]

The trend of the loss factor tan δ is also highly unique (see Figure 3b bottom). Showing a rather broad maximum with a peak at 59 ± 2 °C at dry conditions, the curves become sharper and the maxima are located at 36 ± 2 °C at 25% r.h. and at 21 ± 2 °C at 50% r.h. For 75% r.h., the curve of tan δ shows a steep increase down to 5 °C. The data strongly suggest that the maximum will appear at temperatures well below 5 °C. The loss factor increase results in higher energy dissipation as a function of increasing relative humidity. This is in line with the observed difference of E' between dry and wet conditions. Using the loss factor as evaluation criterion for the glass transition temperature T_g, one can extract the following trend: with increasing humidity, T_g decreases from about 60 °C in dry state to below 5 °C at 75% r.h.
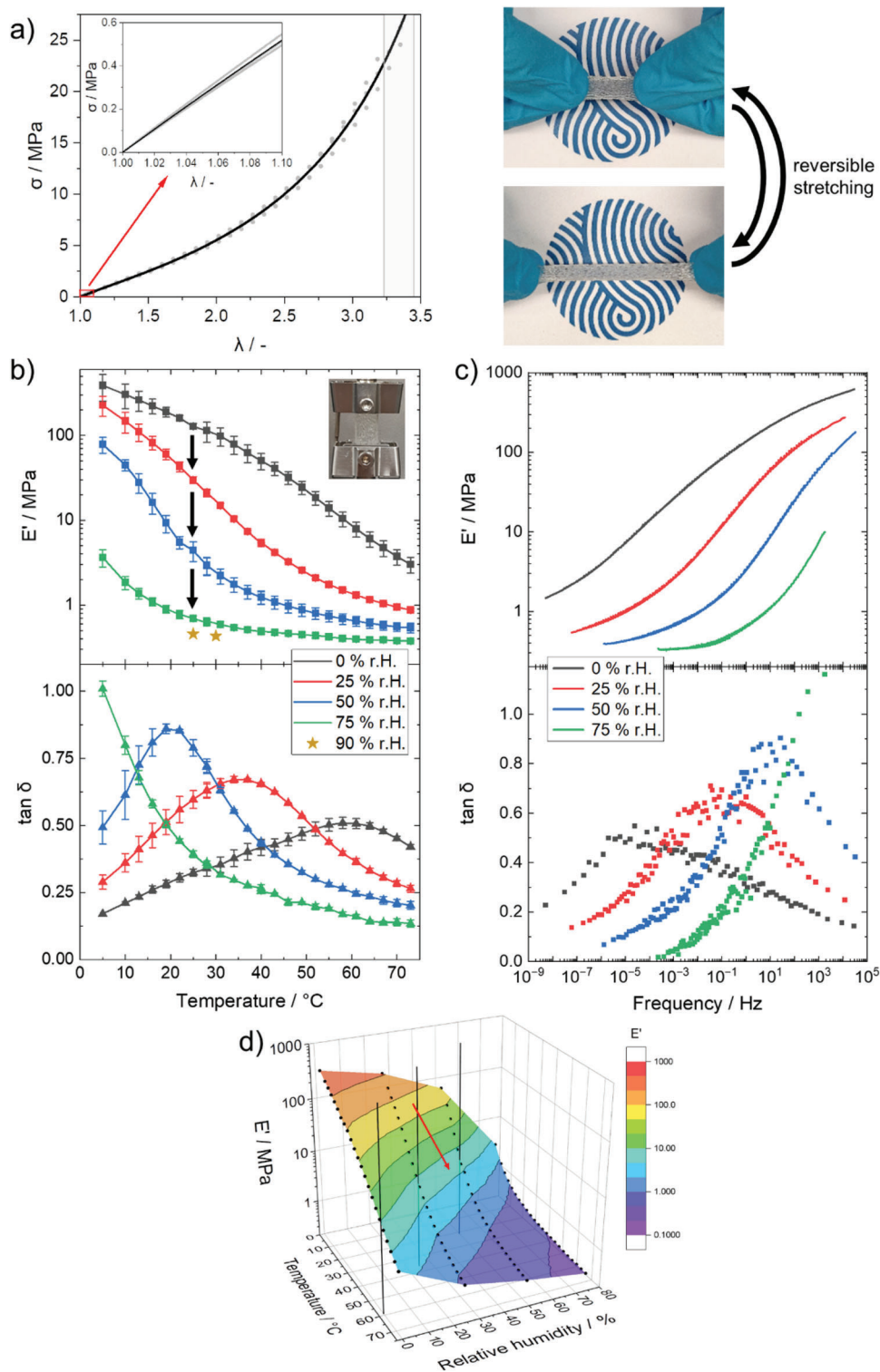
Figure 3. a) Photos highlighting stretching of hydrogel stripe and tensile test of three different samples at ambient conditions (around 20 °C, 45 ± 5% r.h.). Measured with rectangular samples at a strain speed of 10 mm min⁻¹ and fitted with the eight-chain hyperelastic model of Arruda and Boyce. b) Storage modulus E' (top) and loss factor $\tan \delta$ (bottom) for different relative humidities (r.h.) as function of temperature (measured at 1 Hz). The photograph shows the fixation in the DMA apparatus. c) Master curves of E' and $\tan \delta$ shown for different relative humidities at a reference temperature of 25 °C. d) Obtained values from DMA measurements as a function of relative humidity and temperature. Black lines mark the T_g for the respective relative humidity, red arrow marks the area of the steepest decrease of E'.

**ADVANCED
SCIENCE NEWS**

www.advancedsciencenews.com

**ADVANCED
MATERIALS
TECHNOLOGIES**

www.advmattechnol.de

Taking 25 °C as relevant temperature of use, the material shows a T_g above room temperature at 0% and 25% r.h. and behaves like a rather stiff material. Above 50% r.h., the material becomes softer with a T_g below room temperature. The higher the r.h., the lower the T_g. As the material contains hydrophilic amide and ether functional groups, water molecules can diffuse from a humid atmosphere into the material. Water then acts as a kind of plasticizer through hydrogen bonding, this is reported for commodity polymers such as polyamides and polyurethanes.[47,48] The absorbed water lowers the T_g and hence influences mechanical properties significantly.[35,45,49,50]

While Figure 3b represents the material behavior at different temperatures at one selected frequency at 1 Hz, Figure 3c shows master curves at 0%, 25%, 50%, and 75% r.h. for the storage modulus (top) and the loss factor (bottom) which are obtained from frequency sweeps (0.01–10 Hz) at isothermal and isohumid conditions. The horizontal shifting of the frequency data in the master curves clearly suggests that the hydrogels are thermorheological simple materials at all four selected relative humidities. The time–temperature superposition allows for an interpretation of the hydrogel behavior in a large frequency domain at fixed reference temperature. Relaxation times over 14 orders of magnitude are accessible from these data sets (see Figures S11 and S12 in the Supporting Information for further information). This is particularly important for applications in soft robotics where static holding, i.e., long relaxation times, or highly dynamic responses, i.e., short relaxation times, might be required. In terms of skin requirements, the patches have to follow the movements of the body, which involves both, abrupt and slow motions.

3. Conclusion

Summarizing, the temperature- and humidity-dependent water uptake and rheological properties of a new type of hydrogel material have been presented. The material reversibly responds and autonomously adapts to varying environmental conditions— from dry to wet.

Normally brittle and rigid in dry state, NIPAM crosslinked and copolymerized with oligo(ethylene glycol) acrylates show outstanding flexibility and stability at ambient conditions. The glass transition T_g of these smart rubbers is strongly affected by relative humidity and ranges from about 60 °C to temperatures below 0 °C. The hyperelastic stress–strain behavior gives strain-at-break ϵ_b values above 200%. Most interestingly, the stiffness (storage modulus) of the material can be tuned over four orders of magnitude from ≈0.6 up to 400 MPa, compare Figure 3d, by temperature and relative humidity as external triggers.

The effect of strongly differing material stiffness upon changing environmental conditions is highly intriguing for soft robotic and smart skin applications: upon sensing and adapting to temperature and/or relative humidity, large dimensional changes are triggered which can be used for actuating applications. For skin applications, the demonstrated tunable drug release rates will allow for personalized medication, e.g., in wound therapy in the future.

4. Experimental Section

Materials: N-Isopropylacrylamide (NIPAM, purity ≥97%), poly(ethylene glycol)-diacrylate (PEG-DA, M_n 700 g mol^{-1} as confirmed with ^{1}H NMR analysis), triethyleneglycolmonoethylethermethacrylate (TEG-MA, M_n 246 g mol^{-1}), and 2-hydroxy-4′-(2-hydroxyethoxy)-2-methylpropiophenone (photoinitiator, purity ≥98%) were purchased from Sigma-Aldrich (Germany) and used without further purification. Diclofenac sodium, sodium chloride, disodium hydrogen phosphate, potassium dihydrogen phosphate, and potassium chloride were of European Pharmacopoeia grade. Polycarbonate membranes with a pore diameter of 0.03 μm were obtained from Whatman Nuclepore (Global Life Sciences Solutions USA LLC, Marlborough, United States). The commercial patch with diclofenac sodium (Voltaren Schmerzpflaster, GlaxoSmithKline) was purchased from a local pharmacy.

Synthesis: The hydrogel patches were prepared via in situ photopolymerization. First, 1.3 g of NIPAM was ultrasonicated for 10 min in 22 g of purified water (18.2 MΩ) in a 50 mL flask. After dissolving of NIPAM, 1.1488 g of PEG-DA and 0.3018 g of photoinitiator were added to the solution. After stirring the solution for 20 min, 0.792 mL (0.8075 g) of TEG-MA were added. The comonomer ratios correspond to 70 mol% NIPAM, 10 mol% PEG-DA, and 20 mol% TEG-MA. The solution was stirred again for 20 min to ensure complete dissolving and mixing of all components. Then the solution was placed in an ice-water bath and stirred for further 15 min to ensure cooling of the solution. The solution was casted into a pre-cooled PTFE-mold and put under the UV-Lamp (UVItec LF-206LS UV-Lamp (365 nm, Power 6 W)), which was placed 6 cm above the mold. Photopolymerization was carried out for 60 min to obtain a swollen hydrogel. The gel was put into deionized (DI) water and washed for 2 days (with daily water exchange) to remove any unreacted components and impurities. The hydrogels were dried at 60 °C overnight.

Swelling Degree: To determine the swelling degree of the hydrogel material, small pieces (diameter 3 to 6 mm) were punched out of the dry material and dried overnight under vacuum. Afterward, the samples were weighed (m_0), put into 10 mL glass vials which were filled with DI water and then sealed. For the determination of the temperature-dependent swelling degree, the glass vials were put into a temperature-controlled water bath (LAUDA Alpha RA 8). After 24 h, the samples were taken out of the water, carefully blotted on a filter paper to remove surface water and immediately weighed (m_s). The average swelling degree was determined from at least three samples.

Dynamic vapor sorption (DVS) analysis was performed to determine water absorption as function of r.h. and temperature. For this purpose, three round samples (diameter 10 mm) were placed into a DVS analyzer (SPS11, ProUmid) and subjected to the desired measurement protocol. The mass of the samples was determined automatically every 10 min and after reaching the sorption equilibrium ($\Delta m \leq 0.02\%$ per 60 min) it was continued with the next step. Water absorption kinetics were determined for three different temperatures (5, 25, and 60 °C) for different r.h. (25%, 50%, 75%, and 95%). Between the individual temperature cycles, the samples were completely dried. To get information about the temperature-dependent water uptake at 75% r.h., the sample was cooled from 60 to 5 °C in steps of 5 °C. Between each step, the samples were allowed to reach water sorption equilibrium.

Mechanical Characterization: Humidity- and temperature-dependent dynamic-mechanical analysis (DMA) was performed with rectangular samples. The dimensions of the samples were 20 mm long, 10 mm wide, and 1 mm thick. A rheometer (MCR 502 WESP, Anton Paar), equipped with an environmental chamber (CTD 180, Anton Paar) and a humidity generator (MHG 100, ProUmid) was used. The samples were tested by force-controlled extensional rheology with a rectangular fixture system (SRF5, Anton Paar). At first, amplitude sweeps were conducted to determine the linear-viscoelastic area (LVA) of the material (see Figure S10, Supporting Information). Therefore, different force amplitudes were measured at different r.h. and temperatures.

For the force-controlled frequency sweeps, the material was equilibrated for at least 12 h at the desired r.h. at 25 °C. After this step was

**ADVANCED
SCIENCE NEWS**

www.advancedsciencenews.com

**ADVANCED
MATERIALS
TECHNOLOGIES**

www.advmattechnol.de

finished, the sample was cooled to 5 °C and equilibrated for another 6 h. When the equilibration was completed, the frequency sweep was conducted. The mechanical properties of the samples were determined in tension, starting at a temperature of 5 °C, as a function of frequency (0.01 to 10 Hz). After the frequency sweep was completed at the selected temperature, the sample was heated in 3 °C steps to the next temperature level, from 5 to 73 °C.

Stress–strain properties were measured with an Instron 5565 tensile tester, equipped with a 1 kN load cell at a strain speed of 10 mm min^{-1}. Rectangular samples of $\approx 30 \times 10 \times 1$ mm ($l \times w \times t$) were used.

Drug Loading and Release Experiments: For drug loading, the hydrogel was dried for 3 h at 60 °C and afterward stored temporarily over silica to cool down to room temperature (25 °C). The dried gel samples were immersed into a solution of diclofenac sodium in purified water (2.5 g L^{-1}) for 24 h at room temperature to reach the equilibrium state of swelling. After removing the swollen gel from the solution, the water was wiped off with precision wipes. Subsequently, disks were punched out of the gel for further use.

To generate a defined moisture content in the gel, the drug-loaded swollen gel patches were stored at different r.h. (25%, 50%, 75%) for 24 h to reach equilibrium by water diffusion. For the following 6 h release studies, an environmental chamber (CTD 180, Anton Paar) equipped with a humidity generator (MHG 100, ProUmid) was used, while the samples for the following 60 h release studies were conditioned in a climate chamber (ICH-L 110, Memmert). Moisture content in the gels was determined gravimetrically by comparing mass of the gel in equilibrium state and dry state which makes it possible to calculate the degree of swelling.

The in vitro drug release studies were carried out using modified Franz diffusion cells (Gauer Glas, Puettlingen, Germany). The receptor compartment had a volume of 12 mL and was filled with PBS pH 7.4 as receptor medium. The inner diameter of the cell was 15 mm resulting in an effective release area of 1.77 cm^2. The donor and receptor compartments were separated by a polycarbonate membrane. The measurements were conducted at ambient conditions. The receptor medium was degased by ultrasound prior to the studies. The Franz diffusion cells were tempered at 32 °C in a water bath and stirred by means of a magnetic stirring bar with a speed of 500 rpm during the studies.[51]

At the beginning of the measurement and after each hour, 1 mL of the receptor phase was withdrawn through the sampling arm and replaced by fresh pretemperated medium. Sink conditions (concentration <10% of saturation concentration) were maintained over the entire measurement period. The hydrogel patches were weighed both before and immediately after the release experiment to calculate the degree of swelling. Samples were analyzed spectrophotometrically at 276 nm using a microplate reader (Varioskan Lux, Thermo Fisher Scientific GmbH, Germany). Studies were performed in triplicate.

Supporting Information

Supporting Information is available from the Wiley Online Library or from the author.

Acknowledgements

Conflict of Interest

The authors declare no conflict of interest.

Data Availability Statement

The data that support the findings of this study are available from the corresponding author upon reasonable request.

Keywords

[1] D. J. Beebe, J. S. Moore, J. M. Bauer, Q. Yu, R. H. Liu, C. Devadoss, B. H. Jo, *Nature* **2000**, *404*, 588.

[2] F. Ilievski, A. D. Mazzeo, R. F. Shepherd, X. Chen, G. M. Whitesides, *Angew. Chem.* **2011**, *123*, 1930.

[3] D. Rus, M. T. Tolley, *Nature* **2015**, *521*, 467.

[4] L. Ionov, *Mater. Today* **2014**, *17*, 494.

[5] B. Mosadegh, P. Polygerinos, C. Keplinger, S. Wennstedt, R. F. Shepherd, U. Gupta, J. Shim, K. Bertoldi, C. J. Walsh, G. M. Whitesides, *Adv. Funct. Mater.* **2014**, *24*, 2163.

[6] M. Wiese, K. Rustmann, A. Raatz, in 2019 IEEE/RSJ Int. Conf. Intelligent Robots and Systems (IROS), IEEE, Piscataway, NJ **2019**, pp. 7176–7182.

[7] S. R. Eugster, J. Harsch, M. Bartholdt, M. Herrmann, M. Wiese, G. Capobianco, *IEEE Rob. Autom. Lett.* **2022**, *7*, 2471.

[8] J. C. Yang, J. Mun, S. Y. Kwon, S. Park, Z. Bao, S. Park, *Adv. Mater.* **2019**, *31*, 1904765.

[9] A. Ní Annaidh, K. Bruyère, M. Destrade, M. D. Gilchrist, M. Otténio, *J. Mech. Behav. Biomed. Mater.* **2012**, *5*, 139.

[10] M. Ottenio, D. Tran, A. Ní Annaidh, M. D. Gilchrist, K. Bruyère, *J. Mech. Behav. Biomed. Mater.* **2015**, *41*, 241.

[11] M. A. C. Stuart, W. T. S. Huck, J. Genzer, M. Müller, C. Ober, M. Stamm, G. B. Sukhorukov, I. Szleifer, V. V. Tsukruk, M. Urban, F. Winnik, S. Zauscher, I. Luzinov, S. Minko, *Nat. Mater.* **2010**, *9*, 101.

[12] M. Wei, Y. Gao, X. Li, M. J. Serpe, *Polym. Chem.* **2017**, *8*, 127.

[13] S. Minko, *J. Macromol. Sci., Part C: Polym. Rev.* **2006**, *46*, 397.

[14] N. A. Peppas, J. Z. Hilt, A. Khademhosseini, R. Langer, *Adv. Mater.* **2006**, *18*, 1345.

[15] A. Halperin, M. Kröger, F. M. Winnik, *Angew. Chem.* **2015**, *127*, 15558.

[16] H. G. Schild, *Prog. Polym. Sci.* **1992**, *17*, 163.

[17] F. Doberenz, K. Zeng, C. Willems, K. Zhang, T. Groth, *J. Mater. Chem. B* **2020**, *8*, 607.

[18] A. C. C. Rotzetter, C. M. Schumacher, S. B. Bubenhofer, R. N. Grass, L. C. Gerber, M. Zeltner, W. J. Stark, *Adv. Mater.* **2012**, *24*, 5352.

[19] K. H. Son, J. W. Lee, *Materials* **2016**, *9*, 854.

[20] W.-F. Lee, Y.-H. Lin, *J. Mater. Sci.* **2006**, *41*, 7333.

[21] Y. Wu, S. Joseph, N. R. Aluru, *J. Phys. Chem. B* **2009**, *113*, 3512.

[22] Y.-W. Lee, S. Chun, D. Son, X. Hu, M. Schneider, M. Sitti, *Adv. Mater.* **2022**, *34*, 2109325.

[23] M. Hippler, E. Blasco, J. Qu, M. Tanaka, C. Barner-Kowollik, M. Wegener, M. Bastmeyer, *Nat. Commun.* **2019**, *10*, 232.

[24] M. A. Haq, Y. Su, D. Wang, *Mater. Sci. Eng., C* **2017**, *70*, 842.

[25] H. Zhang, Z. Liu, J. Mai, N. Wang, H. Liu, J. Zhong, X. Mai, *Adv. Sci.* **2021**, *8*, 2100320.

**ADVANCED
SCIENCE NEWS**

www.advancedsciencenews.com

**ADVANCED
MATERIALS
TECHNOLOGIES**

www.advmattechnol.de

[26] S. Naficy, H. R. Brown, J. M. Razal, G. M. Spinks, P. G. Whitten, *Aust. J. Chem.* **2011**, *64*, 1007.

[27] L.-W. Xia, R. Xie, X.-J. Ju, W. Wang, Q. Chen, L.-Y. Chu, *Nat. Commun.* **2013**, *4*, 2226.

[28] A. Sidorenko, T. Krupenkin, A. Taylor, P. Fratzl, J. Aizenberg, *Science* **2007**, *315*, 487.

[29] C. Lv, H. Xia, Q. Shi, G. Wang, Y.-S. Wang, Q.-D. Chen, Y.-L. Zhang, L.-Q. Liu, H.-B. Sun, *Adv. Mater. Interfaces* **2017**, *4*, 1601002.

[30] L. Zhang, H. Liang, J. Jacob, P. Naumov, *Nat. Commun.* **2015**, *6*, 7429.

[31] K. Matsumoto, N. Sakikawa, T. Miyata, *Nat. Commun.* **2018**, *9*, 2315.

[32] S. Bhaladhare, S. Kim, K. R. Carter, *ACS Appl. Polym. Mater.* **2019**, *1*, 2846.

[33] H. Okuzaki, K. Hosaka, H. Suzuki, T. Ito, *React. Funct. Polym.* **2013**, *73*, 986.

[34] S. Taccola, F. Greco, E. Sinibaldi, A. Mondini, B. Mazzolai, V. Mattoli, *Adv. Mater.* **2015**, *27*, 1668.

[35] C. Dingler, H. Müller, M. Wieland, D. Fauser, H. Steeb, S. Ludwigs, *Adv. Mater.* **2021**, *33*, 2007982.

[36] D. Segiet, R. Jerusalem, F. Katzenberg, J. C. Tiller, *J. Polym. Sci.* **2020**, *58*, 747.

[37] W.-Y. Chen, M.-Y. Hsu, C.-W. Tsai, Y. Chang, R.-C. Ruaan, W.-H. Kao, E.-W. Huang, H.-Y.-T. C. Chuan, *Langmuir* **2013**, *29*, 4259.

[38] K.-J. Liu, J. L. Parsons, *Macromolecules* **1969**, *2*, 529.

[39] O. E. Philippova, S. I. Kuchanov, I. N. Topchieva, V. A. Kabanov, *Macromolecules* **1985**, *18*, 1628.

[40] M. Thommes, K. Kaneko, A. V. Neimark, J. P. Olivier, F. Rodriguez-Reinoso, J. Rouquerol, K. S. Sing, *Pure Appl. Chem.* **2015**, *87*, 1051.

[41] S. Dodoo, R. Steitz, A. Laschewsky, R. von Klitzing, *Phys. Chem. Chem. Phys.* **2011**, *13*, 10318.

[42] T. Ilić, I. Pantelić, S. Savić, *Pharmaceutics* **2021**, *13*, 710.

[43] T. Canal, N. A. Peppas, *J. Biomed. Mater. Res.* **1989**, *23*, 1183.

[44] R. T. Ju, P. R. Nixon, M. V. Patel, D. M. Tong, *J. Pharm. Sci.* **1995**, *84*, 1464.

[45] G. Baschek, G. Hartwig, F. Zahradnik, *Polymer* **1999**, *40*, 3433.

[46] E. M. Arruda, M. C. Boyce, *J. Mech. Phys. Solids* **1993**, *41*, 389.

[47] L.-T. Lim, I. J. Britt, M. A. Tung, *J. Appl. Polym. Sci.* **1999**, *71*, 197.

[48] D. Fauser, H. Steeb, *J. Mater. Sci.* **2022**, *57*, 9508.

[49] L. Smith, V. Schmitz, *Polymer* **1988**, *29*, 1871.

[50] H. Piao, L. Chen, Y. Kiryu, I. Ohsawa, J. Takahashi, *Fibers Polym.* **2019**, *20*, 611.

[51] D. J. Lunter, R. Daniels, *Eur. J. Pharm. Biopharm.* **2012**, *82*, 291.